Determining the Kerr constant in optically isotropic liquid crystals

Tetiana Yevchenko ®,* Dorota Dardas ®,† Wojciech Kuczyński, and Arkadiusz C. Brańka ®‡

Institute of Molecular Physics, Polish Academy of Sciences, M. Smoluchowskiego 17, 60-179 Poznań, Poland

A new scheme is investigated for evaluating the temperature dependence and dispersion relation of the Kerr constant (K) of an optically isotropic medium in isotropic and blue phases (BPs) liquid crystals. The scheme employs the measurement of the component of the transmitted light intensity of double modulated frequency using the modified in-plane-switching cell geometry (based on metallic film electrodes). It overcomes to a large extent the problem of a nonuniform electric field, employs relatively small driving voltages, and allows K to be measured directly. It is shown that the dispersion relation based on the single-band birefringence model describes well both blue and isotropic liquid crystal phases. It is found that the experimental data indicate that the temperature-dependent coefficients in this relation have a simple linear form in the isotropic phase, which allows a general model for the temperature and wavelength dependence of the Kerr constant in the isotropic liquid crystal phase to be formulated. In the BPs the temperature dependence of the experimental data deviate from the simple linear trend, but follow well an inverse exponential form.

I. INTRODUCTION

The Kerr effect is a well-known quadratic electro-optical phenomenon (QEO) in which a change in the refractive index of a material is induced in response to an applied electric field. This effect is present in any dielectric material but usually is obscured by a stronger first-order effect. However, in an isotropic medium such as liquids, isotropic liquid crystal (LC) composites, BPs, and crystals with centrosymmetric point groups, the first-order effects are canceled by symmetry and the dominant effect becomes the QEO effect. Thus, an optically isotropic medium under the influence of an electric field becomes optically anisotropic or birefringent with the optical axis parallel to the electric field direction. The induced birefringence is directly proportional to the square of the electric field and the difference in index of refraction is given by

$$\Delta n_{\text{ind}} = \lambda K E^2, \tag{1}$$

where λ is the wavelength of the incident light, K is the Kerr constant, and E is the intensity of the electric field. The Kerr phenomenon is the basic physical mechanism of electro-optical properties of liquid crystal blue phases, which means the Kerr constant constitutes one of the central quantities in the liquid crystal field.

Blue phases are unique liquid crystals which form frustrated structures with crystal (cubic) symmetry. In these structures chiral nematic molecules are self-assembled in double twist helixes or cylinders which are separated by defect regions (disclinations). Defects are ordered in a 3D periodic structure with a typical lattice spacing of the order of several hundred nanometers [1,2]. Three types of BPs are known: amorphous BPIII and two phases organized in a cubic fashion, which are simple cubic BPII and body-centered cubic BPI. They are formed typically between the isotropic and cholesteric phases in a narrow temperature range, although structural modifications have been made which have extended their temperature stability ranges considerably [3]. This revived interest in blue phase research, is in part because of possible applications in next-generation displays in which the operation mechanism is based on a Kerr effect-induced isotropic-to-anisotropic transition. This is qualitatively different from nematic liquid crystal displays (LCD) which exploit the LC director reorientation [4]. Potential applications of BP liquid crystals are based on their optical isotropy and the fact that the Kerr effect is fast, and submillisecond response times could be achieved. Also, liquid crystalline blue phases exhibit a relatively large Kerr constant [4–6] which can be exploited directly to reduce the driving voltage.

Strictly speaking the Kerr constant of a medium is not a constant but can be affected by various factors, in particular temperature (T) and light wavelength (λ). Also, the measurement of this important physical quantity still remains far from being routine, particularly in the case of BPs. Further progress in the development of BP-based devices largely rely on a better understanding of how different factors influence K and on the development of efficient and accurate methods for its determination.

Historically, the basic means to determine Kerr constants has been a Kerr cell [5,7]. In the Kerr cell the relation in Eq. (1) is utilized and a uniform electric field is produced which is a great advantage of this approach. However, to measure K large driving voltages have to be employed and a relatively large sample is required to perform the experiment. Thus, this method is usually employed to study the Kerr

---

*yevchenko@ifmpan.poznan.pl
†Corresponding author: dardas@ifmpan.poznan.pl
‡branka@ifmpan.poznan.pl

effect in isotropic liquids and liquid crystals above the clearing point [5,8].

Because, in experiments and display applications, the LC layer is typically sandwiched between two planes, the in-plane-switching (IPS) cell configuration is often the chosen approach to determine Kerr constants of LC materials. For measurements of the electro-optical Kerr effect in IPS, comb-type interdigitated electrodes are often used. In this way the electric field is mainly in the lateral direction which is consistent with the requirement that the induced birefringence should be parallel to the cell substrates to determine K. However, the electric field produced is spatially nonuniform (apart from a tiny strip between electrodes) which is the main disadvantage of such IPS measurements. To reduce the problem of field nonuniformity, different IPS configurations have been proposed (e.g., etched or protruded electrode IPS [4,9–11]) but none of these can be considered to be fully satisfactory. Some of these ideas are at the modeling stage and may be difficult to apply in practice. Also, in these IPS modifications the focus was mainly on improving the performance of the LCD structure and not on the measurement of K itself. Furthermore, in the IPS geometry, for practical reasons, the most uniform part of field has been taken into account, e.g., via a scaling factor or by considering effective values [12,13].

To overcome the drawbacks of both the IPS and Kerr cell methods, vertical field switching (VFS) devices were proposed [14,15], in which the electric field is along the longitudinal direction and is uniform on application of comparatively small driving voltages. Another advantage of the VFS mode is that it is possible to reduce hysteresis effects. However, the measurement method exploits the matrix fitting stage and the device construction in the VFS mode is much more sophisticated than in an IPS cell, which can affect its performance. For example, the dependence of the Kerr constant on the cell gap is know to occur in the VFS cell [16].

Another approach to determine K is the extended Kerr effect which was proposed to describe the saturation phenomenon in the refractive index change as the electric field increases. This phenomenon has been formulated in terms of a two-parameter exponential formula which reduces to the Kerr effect in Eq. (1) in the low electric field region [17,18]. This phenomenological approach requires large driving voltages and has proved useful in the analysis of electro-optical properties of polymer stabilized optically isotropic LC [4]. The extended Kerr formulation is also exploited in this work.

The aim of this work is to obtain a more comprehensive description of the effects of T and λ on the constant K in optically isotropic liquid crystals. To achieve it we propose a new approach in which the main problem of the nonuniformity of the electric field in the IPS configuration can be reduced and the K-value be determined directly without any additional approximations or scaling factors. The proposed approach combines the measurement of the modulated AC component of the transmittance intensity with a simple IPS cell design comprising two metallic films acting as electrodes.

The idea to use cells with metallic films was exploited previously in Refs. [19,20] to study order-disorder transitions in LC and recently in Ref. [21] to generate second harmonics in nematic liquid crystals. In these measurements large driving voltages were needed and relatively thick samples were used.
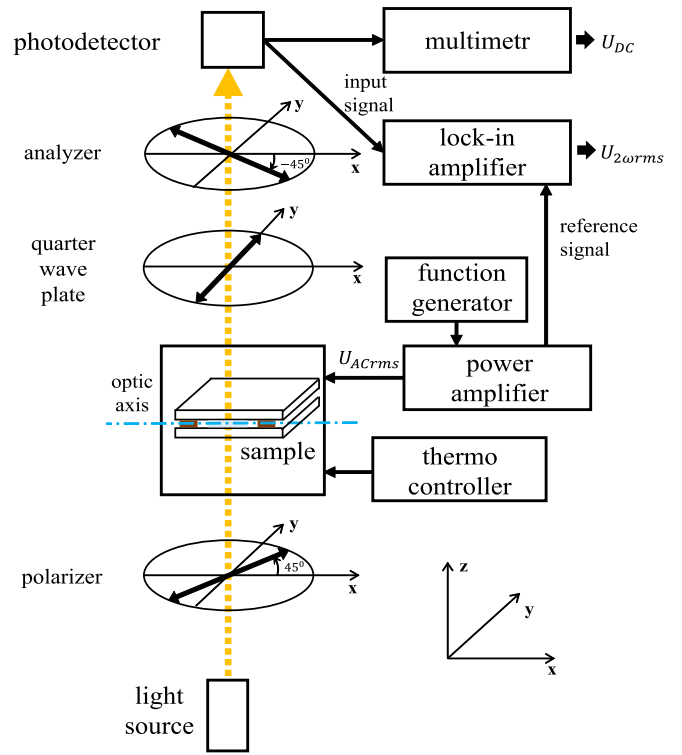

FIG. 1. The scheme of the measuring system of determination the electro-optical Kerr effect.

In the proposed approach described here lower field and thinner layers are used which is a significant factor in the accurate determination of the Kerr constant of liquid crystals BPs.

The work is organized as follows. In Sec. II the method for determinig the Kerr constant is described. The experimental details and materials used are given in Sec. III. In Sec. IV the results are presented and discussed. The temperature and dispersion relations of the Kerr constants are analyzed. The main conclusions are summarized in Sec. V.

II. METHOD

The proposed method for determining the Kerr constant is described below and the corresponding measurement setup is shown schematically in Fig. 1.

When a uniaxial medium is placed between a polarizer and analyzer the light intensity transmitted by the system is [22]

$$I = I_0 \left[\cos^2 \gamma - \sin (2\alpha) \sin (2\beta) \sin^2 \frac{\delta}{2} \right], \quad (2)$$

where α and β are the angles between the optical axis of the sample and the polarization directions of polarizer and analyzer, respectively. The angle, γ is the difference, $\alpha - \beta$. When the polarizer and analyzer are crossed $\gamma = \pi/2$. The incident light intensity is I_0, and δ denotes the phase lag (retardation) between the ordinary and extraordinary rays after passing through the sample. If we deal with the optically isotropic sample under an applied electric field, and additionally a quarter-wave plate is placed between the sample and the

analyzer (as in Fig. 1), then the retardation is

$$\delta = \frac{2\pi d \Delta n_{\text{ind}}}{\lambda} + \frac{\pi}{2}, \qquad (3)$$

where Δn_{ind} is the induced birefringence and d denotes the sample thickness. Providing, an external alternating electric field, $E = E_{\text{AC}} \cos \omega t$, is applied, the polarizer and analyzer are crossed, and the quarter waveplate forms the angle $\pi/4$ with the analyzer, then from Eqs. (2) and (3),

$$
\begin{aligned}
\frac{I}{I_0} &= \sin^2 \left(\frac{\pi}{4} + \frac{\pi d \Delta n_{\text{ind}}}{\lambda} \right) \\
&= \sin^2 \left(\frac{\pi}{4} + \pi d K E_{\text{AC}}^2 \cos^2 \omega t \right) \\
&= \frac{1}{2} \left(\sin \left(2\pi d K E_{\text{AC}}^2 \cos^2 \omega t \right) + 1 \right),
\end{aligned} \qquad (4)
$$

where Eq. (1) was used in the second equality. The last expression follows from the trigonometric relation, $\sin^2(\pi/4 + x) = [\sin(2x) + 1]/2$. It is important to note that the argument of the sin function in this expression is very small (mainly due to the small value of K), so as $\sin(x << 1) \cong x$ the following relation holds to a good approximation,

$$\frac{I}{I_0} \cong \frac{1}{2} + \pi d K E_{AC}^2 \cos^2 \omega t. \qquad (5)$$

Then, using the trigonometric identity $\cos^2(x) = \frac{1}{2}[1 + \cos(2x)]$ the above expression can be transformed to the form

$$\frac{I}{I_0} \cong \frac{1}{2} + \frac{1}{2}\pi d K E_{AC}^2 + \frac{1}{2}\pi d K E_{AC}^2 \cos 2\omega t. \qquad (6)$$

Equation (6) indicates that the ratio I/I_0 is the sum of two terms in which $I_{\text{DC}}/I_0 = \frac{1}{2} + \frac{1}{2}\pi d K E_{\text{AC}}^2 \cong \frac{1}{2}$ is the constant component of the light intensity and $I_{2\omega}/I_0 = \frac{1}{2}\pi d K E_{\text{AC}}^2$ is the component of double modulation frequency of light intensity. There is no component of the light intensity with the basic modulation frequency ω (i.e., $\frac{I_{1\omega}}{I_0} \equiv 0$) and it is the quarter-wave plate which introduces the Kerr effect in the form of the light modulation at the second harmonic of the electric field.

These two components of the light intensity, provide sufficient information for the determination of K. Notably, taking into account the fact that the intensity of the transmitted light is measured by a photodetector, where the resulting voltage is proportional to the light intensity (the linear range is considered only [23]), we obtain the following relation:

$$\frac{I_{2\omega}}{I_{\text{DC}}} = \frac{U_{2\omega}}{U_{\text{DC}}} = \pi d K E_{\text{AC}}^2, \qquad (7)$$

where $U_{2\omega}$ and U_{DC} are the voltages corresponding to measurements at double the detection frequency and the constant component of the electric field, respectively. From the above expression the formula for the Kerr constant is

$$K = \frac{U_{2\omega}}{\pi d U_{\text{DC}} E_{\text{AC}}^2}. \qquad (8)$$

Let $E_{\text{AC}} = U_{\text{AC}}/l$, where U_{AC} is the voltage applied to the sample and l denotes the distance between the electrodes. The voltages from the instruments in rms values are, $U_{2\omega} = U_{2\omega\text{rms}} \cdot \sqrt{2}$ and $U_{\text{AC}} = U_{\text{ACrms}} \cdot \sqrt{2}$. The final formula which

is used in the measuring system in Fig. 1 is

$$K = \frac{U_{2\omega\text{rms}} l^2 \sqrt{2}}{2\pi d U_{\text{DC}} U_{\text{ACrms}}^2}. \qquad (9)$$

The linear relationship between $U_{2\omega\text{rms}}$ and U_{ACrms}^2, i.e., $U_{2\omega\text{rms}} = \mathbb{A} U_{\text{ACrms}}^2$ where $\mathbb{A} = \sqrt{2}\pi d K U_{\text{DC}}/l^2$ is a slope constant, provides a simple and useful test for the correctness of the measuring procedure. Using the slope $\mathbb{A}$, the Kerr constant can be obtained from the following expression:

$$K = \mathbb{A} \frac{l^2}{\sqrt{2}\pi d U_{\text{DC}}}. \qquad (10)$$

The measurement setup shown schematically in Fig. 1 for the electro-optical Kerr effect, which enables a direct determination of K with Eq. (9) [or Eq. (10)], makes use of the IPS cell geometry and requires only a few commonly available devices (hot-stage, electric field generator to provide U_{ACrms}-voltage, photodetector, multimeter to measure U_{DC}-voltage and lock-in amplifier to register $U_{2\omega\text{rms}}$-voltage). An essential part of the proposed scheme is the IPS cell, which we refer to here specifically as the IPSm cell, consists of two metallic films. The films are placed between glass plates and act both as parallel electrodes and spacers. The sample material is placed in the gap between the electrodes. In such a cell geometry the electric field is to a large extent uniform. In this way, the transformation from Eq. (8) to Eq. (9) is obeyed. When the electric field is turned on the induced optical axis it forms an angle $\pm 45°$ with the plane of the polarizer and analyzer, respectively.

Also, as mentioned above, an important element of the scheme is a quarter-wave plate because the transmission component $I_{2\omega}$ then becomes relevant and can be exploited. As this component is proportional to the phase shift between the extraordinary and ordinary ray (retardation) induced by the electric field, a low-value retardation can be determined. Thus, it can be expected that relatively small driving voltages are sufficient to determine K from the proposed scheme. Also, in addition to providing uniform electric fields with the IPSm cell, the scheme allows the simultaneous observation of the sample texture. This is a great advantage which allows phase control and the accurate exploration of transition regions.

III. MATERIALS AND EXPERIMENTAL DETAILS

To validate the proposed approach a well-known nematic liquid crystal, 5CB (4-cyano-4′-pentylbiphenyl) and a mixture of 5CB with 20 mol % of chiral dopant CE2 [4′/-(2-methylbutylphenyl)-4′-(2-methylbutyl)-4-biphenylcarboxylate (Merck)] were used. These materials were selected because the Kerr cell and VSF results are available for these materials and can therefore provide benchmark systems. The 5CB/CE2 mixture, which we will denote as M2, has both BPI and BPII phases and is known to exhibit a large Kerr constant [15].

A sample was placed in the IPSm cell, which was held in a hot stage equipped with a proportional-integral-derivative controller PID UNIPAN type 650 (Scientific Instruments). The temperature was stabilized with an accuracy of ± 0.05 °C. As a source of light, a luminescent interchangeable diode

(LED) was utilized. Additionally, to obtain a monochromatic light source an appropriate filter was placed after the diode. To analyze the influence of the wavelength factor, measurements were carried out with three light wavelengths $\lambda_1 = 532$ nm, $\lambda_2 = 589$ nm, and $\lambda_3 = 633$ nm.

A 1 kHz sine-wave AC signal was applied to the sample, using a synthesized function generator DS340 (Stanford Research Systems Inc.) with a broadband linear amplifier F20A (FLC Electronics). In all of our measurements the voltage U_{ACrms} was less than 100 V.

As shown in Fig. 1 the sample on the hot stage was placed in the path of the light wave beam between polarizers and optical axis of the sample which forms an angle of $\pm45°$ with the plane of the polarizer and the analyzer, respectively. A wavelength-compatible quarter-wave plate (Eksma Optics) was placed between the sample and the analyzer with its axis $45°$ with respect to the analyzer plane. The light intensity was detected by a photodiode Si PiN (Femto). Then, the signal proportional to the light intensity was passed to a digital multimeter 34401A (Hewlett Packard) and to a lock-in amplifier Sr530 (Stanford Research Systems). The DC component U_{DC} of the signal was measured with the multimeter and the second harmonic $U_{2\text{wrms}}$ was determined using the lock-in amplifier.

The IPSm cells for measurements were made from two cut glass plates made from microscope slides. The size of the bottom glass plate was 2.5 cm $\times$ 2.5 cm and the size of the top glass plate was 1.2 cm $\times$ 2.5 cm. Two Cu film electrodes with a thickness d were placed between the glass slides. It was checked in the isotropic phase (5CB, M2) that cells with different electrode widths ($d = 10, 20, 30$ μm) yielded practically the same results. Consequently, in the work, the results are mostly for one $d = 20$ μm value.

The applied electrodes are assumed to produce a uniform electric field $E = U/l$ but, as their intersections are strips and not parallel charged surfaces of infinite extent, some limitations in the applicability of this relation may appear. For example, in practice, the distance between the electrodes cannot be arbitrarily large. Thus, $l < l_{\text{max}}$ where the limiting distance l_{max} slightly depends of the applied voltage and the width of the electrode, and it can be readily established with the linearity criterion from Eq. (10). In this way it was found that for the conditions and cases considered in this work, l_{max} was always less than 10^3 μm. Also, the distance cannot be too small to accommodate a sufficient amount of the LC material. The most suitable distance between the electrodes was found to be in the range 300–900 μm. In the measurements the cells with $l = 500$–700 μm were used.

The values of the Kerr constant determined have an uncertainty of a few percent (up to 10 percent). The uncertainty depends on the quality of the sample cell and the measuring devices. The main systematic contribution is due to the uncertainty in determining the thickness of the electrodes d and the distance l between them (the error contribution of the U_{DC} is about 2 percent). The statistical error of the slope, $\mathbb{A}$, is less than 3 percent and in the figures only this error is given.

IV. RESULTS AND DISCUSSION

The first test of the new method was to see if there is a linear relationship between the resultant $U_{2\omega\text{rms}}$ and the applied
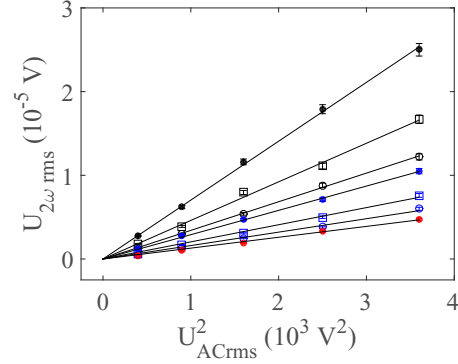

FIG. 2. Test of the relation in Eq. (9). The results (symbols) are for the 5CB in isotropic liquid phase for different temperatures relative to the clearing temperature (from top to bottom $T - T_c = 0.5, 1, 2, 3, 4, 6, 8, 10$ °C). The solid lines are linear fits to the data.

U_{ACrms}^2. The results obtained for 5CB in the isotropic phase for a range of different temperatures are shown in Fig. 2. The data follows well a linear relationship, demonstrating the correctness of the measuring scheme. Any deviation from the linear behavior signals inaccuracies in the measurement procedure or that some of the assumptions in the equation derivation are not fully valid. This useful test was always performed in this work and the slope was used to get K in accordance with Eq. (10).

The Kerr constant for 5CB and the mixture M2 in the isotropic phase (i.e., above their clearing temperatures) are shown in Fig. 3. In the figure the temperature dependence of the inverse of the Kerr constant is compared with values obtained from the VFS [15] and the Kerr cell methods [24,25]. As is evident the data produced by the different methods are in excellent agreement, which validates the new procedures
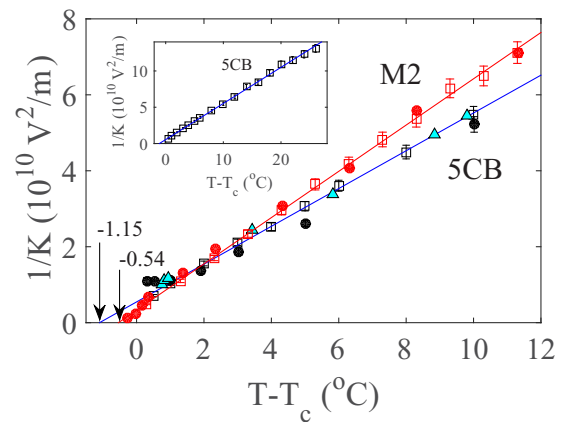

FIG. 3. The inverse of the Kerr constant of 5CB and M2 as a function of temperature, $T - T_c$ in the isotropic phase. The square symbols are results of this work, where the sample thickness was, $d = 20$ μm, $\lambda = 589$ nm, and the distance between the electrodes was, $l = 515$ μm. The filled-in circles and triangles are data from Refs. [15,24]. Lines are the linear fits to the data of this work and the arrows indicate the corresponding temperature difference $T^* - T_c$. The inset shows the results for the same sample, measured over a wider temperature range.

used. Also, the results for higher temperatures shown in the inset of Fig. 3 demonstrates that the measurement arrangement shown on Fig. 1 enables Kerr constant values less than 10^{-11}mV^{-2} to be determined. The ability to determine the Kerr constant over such a wide range of values is a significant advantage of the proposed scheme.

A. Temperature relation

The temperature dependence of K is of great relevance and of fundamental importance. In the liquid state the linear dependence,

$$\frac{1}{K} = (T - T^*)/C, \tag{11}$$

where C is a constant, is well documented for many materials and a general consensus exists that the Landau-de Gennes theory describes well this relationship, at least for temperatures not too close to the clearing temperature, T_c. In this region deviations from the linear prediction have been reported by some authors [25].

As may be seen in Fig. 3 the linear temperature dependence is also well confirmed by this work's data. In all measured cases (also for different λ) the extrapolated constant T^* or the second-order pretransitional temperature, is slightly lower than the respective clearing transition temperature in accordance with the Landau–de Gennes model [2,26].

Changing the amount of chiral dopant can significantly influence the properties of BPs, which is exploited as one of the possible mechanisms to change the K value. The presence of CE2 in 5CB causes that Kerr constant close to the clearing temperature to be larger in the mixture than in pure 5CB. In addition, the dopant causes a faster decrease of K with temperature (i.e., a larger slope of $1/K$ data) and hence at a certain temperature the inverse trend is observed, i.e., the value of K of M2 becomes lower than K of 5CB. Such behavior was also observed for the mixture of 5CB with 42.4 mol % of chiral dopant CE2 (M4). Consequently, we observe the more chiral dopant there is in the mixture the more T^* shifts toward T_c: $T^* - T_c \approx -1.15, -0.54, -0.1 \,^\circ\text{C}$ for 5CB, M2, M4, respectively. The measured clearing point of the mixture M2 (58.5 $\pm$ 0.05 $^\circ$C) and 5CB (35.1 $\pm$ 0.05 $^\circ$C) is given in the brackets.

The temperature dependence of K in the M2 mixture across its BPs is shown in Fig. 4. The range of BPII is about 0.75 $^\circ$C and this result was verified additionally in different commercial IPS cells ($d = 10, 20 \,\mu$m) with the polarizing optical microscope and with the thermooptical analysis [27]. As seen in the figure the form of $K(T)$ and the range of its values are the same as from the VSF measurments in Ref. [15]. The slight difference in the BPII temperature ranges may originate from differences in the cell construction and/or different initial sample treatments. As is known these factors, in particular a monodomain versus multidomains alignment in the sample, can influence the temperature range of BPs [28,29].

In the case of the BPs the form of $K(T)$ is much less well known. A useful formula in the present context has been proposed by Rao, Yan, and Wu [30]. Considering Gerber's formula [31] for K, these authors proposed that the Kerr constant in the BP should vary approximately linearly with
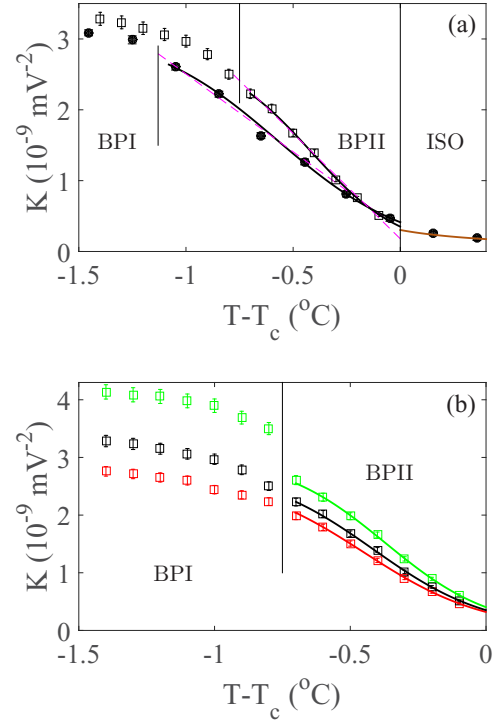

FIG. 4. The Kerr constant as a function of temperature in the BPs and isotropic phase in the M2 mixture. The open squares give results from the present work, and the filled circles show data from Ref. [15] ($\lambda_2 = 589$ nm). In panel (a) the solid and dashed lines represent fits to Eqs. (13) and (14), respectively. The vertical bars indicate the estimated transition temperature between the BPI and BPII phases. The solid line in the ISO phase is from Fig. 3. In panel (b) the results obtained for different wavelengths $\lambda_1 = 532$ nm (green), $\lambda_2 = 589$ nm (black), $\lambda_3 = 633$ nm (red) are shown. The solid lines are the corresponding fits to Eq. (13).

reciprocal temperature $(1/T)$ as

$$K = \zeta \left(\frac{1}{T} - \frac{1}{T_c} \right), \tag{12}$$

where ζ is the proportionality constant. This phenomenological formula can describe the experimental BPII data (the thin dashed line in Fig. 4) and used to estimate the clearing point quite well [6,15], which may be surprising taking into account that the formula only has one free parameter. Close inspection of the data suggests that the dependence in Eq. (12) may only be an approximation. Indeed, plotting $\log(1/K - W)$ versus $T - T_c$ the data follows a straight line for a certain value of the constant W. It means, for the data considered, K is described by

$$K \cong \frac{1}{D \exp[-\eta(T - T_c)] + W}, \tag{13}$$

where η and D are constants. Thus, to obtain a more accurate representation of temperature dependence of K for the BPII at least three parameters are required. Then the formula predicts a nonzero value of the Kerr constant at T_c, $K(T_c) = 1/(D + W)$. The constants D, W are in $1/K$ units, i.e., V^2/m and η in $^\circ\text{C}^{-1}$. For our BPII data in Fig. 4 the constants $(W \times 10^{-9}, D \times 10^{-9}, \eta)$

for $\lambda_1, \lambda_2, \lambda_3$, respectively, are $(0.330, 2.1527, -5.0655)$, $(0.355, 2.4961, -4.690)$, $(0.370, 2.7586, -4.4732)$, and for the data from Ref. [15] they are $(0.319, 2.4762, -3.2912)$. It should be noted that the formula in Eq. (13) is not unique and more experiments with other materials is needed to check its generality.

The formula in Eq. (13) represented by bold solid lines in Fig. 4, traces out the experimental points very well, revealing their slight systematic departures from the linear trend. This means that the Kerr constant, K can also be represented by a simple linear dependence which in particular can be expressed as

$$K \approx \frac{\zeta}{T^{**}}\left(1 - \frac{T}{T^{**}}\right) \quad (14)$$

$$\cong \frac{\zeta}{T^{**}\left(1 - \frac{\Delta T^{**}}{T^{**}}\right)} - \frac{\zeta}{T^{**}} = \zeta\left(\frac{1}{T} - \frac{1}{T^{**}}\right), \quad (15)$$

where T^{**} is a constant close to T_c, $\Delta T^{**} = T^{**} - T$ and as $x = \Delta T^{**}/T^{**} \ll 1$ the relation $1 + x \cong (1 - x)^{-1}$ is well obeyed and has been used in going from Eqs. (14) and (15). It is to be noted that T^{**} for K and the BPII-Iso transition is similar to the T^* for $1/K$ in Iso-BPII transition in that both are linearly extrapolated constants close to T_c [see Eqs. (14) and (11)]. However, the physical meaning of T^{**}, unlike T^*, has not yet been established. For $T^{**} \cong T_c$ the approximation in Eq. (15) becomes the formula in Eq. (12). Thus, in general, two parameters are needed to represent $K(T)$ in the linear approximation, and $K(T_c) \approx \zeta(T^{**} - T_c)/T^{**}$ in this approximation.

The experimental data obtained, along with the linear $K(T)$ forms, shows that the Kerr constant can be slightly discontinuous at the transition to the isotropic liquid phase. Another scenario is that departure from a straight line dependence of $1/K(T)$ in the fluid for small $T - T_c \equiv \Delta T > 0$ takes place [25], which would reduce or even eliminate the discontinuity. It is evident that more studies of K close to the transition region or $|\Delta T| < 0.2\ ^\circ$C, are needed to help resolve these issues.

The data in Fig. 4 show, the $K(T)$ in BPI is also approximately linear, at least for T not too close to the transition region. There is an abrupt change in slope, however, i.e., the K can change much less rapidly with temperature in BPI than in BPII, which is a desirable feature for display applications [32]. The precise description of the data may require the formula like in Eq. (13) but the accuracy of the experimental data does not allow a definite conclusion on this matter. Also, for temperatures near the transition a departure from linearity (where the points smoothly drop down toward BPII K-values) is clearly seen. Nevertheless, at the BPI-BPII boundary a small discontinuity in K cannot be excluded. Also, it would be consistent with previous observations on other properties at the transition temperature [33,34]. We think that this phenomenon deserves further investigation.

B. Dispersion relation

As was noticed above even though K is often referred to as being a "constant," it is a complicated physical property which depends implicitly on many factors such as temperature or material composition. A comprehensive description of K is

not available as yet, however. In what follows we exploit advantages of the proposed scheme to investigate one important and hardly studied issue, namely, the light wavelength dependence or dispersion of K. There are not many reports dealing with the dispersion of K for liquid crystals and in particular for BP materials even though in designing LC-based devices dispersion have to be taken into account. Also, knowledge of the λ dependence of K is a step toward establishing a more explicit formula for $K(T, \lambda)$.

For a polymer-stabilized optically isotropic liquid crystal an approach to describe the dispersion of the Kerr constant has been proposed by Jiao, Yan, and Wu [35]. In their approach, as a starting point, the phenomenological extended Kerr effect model [17,18] was used to calculate the induced birefringence

$$\Delta n_{\rm ind} = \Delta n_s\{1 - \exp[-(E/E_s)^2]\}, \quad (16)$$

where two parameters Δn_s and E_s have the meaning of the saturated induced birefringence and the saturation electric field, respectively. In the low electric-field region $E/E_s \ll 1$, and then this extended Kerr effect reduces to the Kerr effect formula in Eq. (1) and

$$K = \Delta n_s/\lambda E_s^2. \quad (17)$$

The key step was to exploit the single-band birefringence dispersion model [36] and apply it to the saturated induced birefringence, $\Delta n_s = G\lambda^2\lambda^{*2}/(\lambda^2 - \lambda^{*2})$, where λ^* is the wavelength of the nearest absorption band of the LC composite and G is a proportionality constant [36]. This way, via Eq. (17), the following dispersion relation of the Kerr constant for a given temperature was proposed [35]:

$$K = \frac{A\lambda}{\lambda^2 - B}, \quad (18)$$

where $A = \lambda^{*2}G/E_s^2$ and $B = \lambda^{*2}$. For a given temperature, the dispersion dependence can be estimated by exploiting the extended Kerr model [in Eq. (16)] and by suitable fitting of the voltage-dependent transmittance (V-T) curves measured at different wavelengths [35].

The above dispersion formula in Eq. (18) in which $B = \lambda^{*2}$ was shown to describe well the experimental data in the case of a polymer-stabilized LC composite [35]. Its applicability to a broader spectrum of optically isotropic LC at different temperatures is thus of considerable interest. Also, it is to be noted that the Kerr constant in Eq. (18) in this case is the product of a temperature-dependent Kerr coefficient $K(T) = A$ and a wavelengths-dependent $K(\lambda) = \lambda/(\lambda^2 - \lambda^{*2})$ part. We found that a slightly better agreement between experimental data and the formula in Eq. (18) can be achieved if another, more general single-band birefringence dispersion model [37,38] is applied to the saturated induced birefringence, $\Delta n_s = [\sqrt{G_\parallel\lambda^2 - 1} - \sqrt{G_\perp\lambda^2 - 1}]/\sqrt{G_c\lambda^2 - 1}$, where the parameters $G_\parallel, G_\perp, G_c$ depend on the LC material parameters, and the temperature (see the Appendix). The model is based on Vuka's relationship without extra approximations and does not need the resonance wavelength λ^* to calculate the dispersion [37]. It is shown in the Appendix that this model of Δn_s in good approximation, yields the dispersion relation in Eq. (18) in which both $A = [\sqrt{G_\parallel} - \sqrt{G_\perp}]/2\sqrt{G_c}E_s^2$ and $B = 1/2G_c$ are the material- and temperature-dependent parameters. This
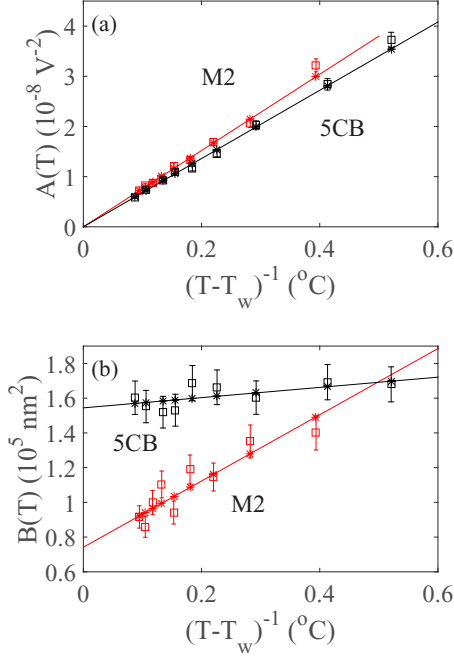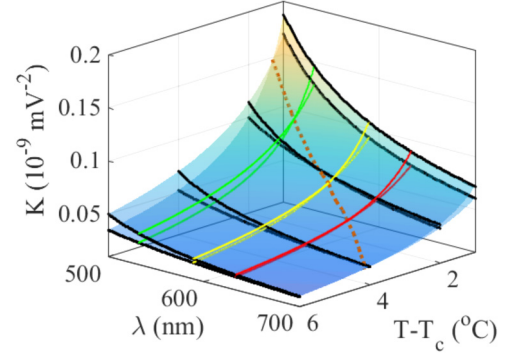
FIG. 6. Temperature and dispersion dependence of the Kerr constant, $K(T, \lambda)$, in the isotropic liquid phase of the 5CB and M2 mixture. The green, yellow, and red lines marked are $K(T)$ for three wavelengths at which measurements were conducted and solid black lines are examples of $K(\lambda)$. The surface is given by relations in Eqs. (18)–(20) with (a_1, b_1, b_2, T_w) given in Fig. 5. The dashed line marks the intersection between the surfaces.

FIG. 5. Parameter A [panel (a)] and parameter B [panel (b)] in Eq. (18) as a function of $(T - T_w)^{-1}$ in the isotropic liquid phases in the 5CB (symbols in black) and M2 mixture (symbols in red). Open circles are from direct fitting of the experimental data. The star symbols are from the linear relation Eq. (11) (solid lines in Fig. 3) for each λ obtained for the same data. The solid line is the linear fit to the star symbols with Eqs. (19) and (20) in panels (a) and (b), respectively. The resultant constants (a_1, b_1, b_2, T_w) are for 5CB $(6.8044 \times 10^{-8}, 29\,465, 154\,420, -1.42)$ and for M2 $(7.6007 \times 10^{-8}, 190\,700, 74\,154, -1.24)$.

is a notable result which shows that in general $K(T, \lambda)$ cannot be represented by the simple product $K(T)K(\lambda)$. The scheme proposed in this work generates sufficiently accurate data to determine the A, B parameters which allows a more comprehensive description of $K(T, \lambda)$ to be made, and to obtain some information on $G_\parallel$, $G_\perp$, G_c, e.g., from the B, the parameter G_c is directly estimated.

Employing the scheme in Sec. II the Kerr constant for three wavelengths ($\lambda_1 = 532$ nm, $\lambda_2 = 589$ nm, and $\lambda_3 = 633$ nm) has been measured for the M2 mixture in their isotropic and BP phases. Also, the corresponding measurements for 5CB liquid, which can be considered to be a limiting case of zero amount of the dopant, were performed. It was verified that in the isotropic phase the dispersion relation formula is well obeyed for each temperature studied and for each wavelength the linear temperature dependence in Eq. (11) holds well (at least for $\Delta T > 0.2\,°C$). The results show that the applicability of the dispersion relation in Eq. (18) is not limited to polymer-stabilized liquid crystal blue phases, but may also describe $K(T, \lambda)$ of other optically-isotropic medium where the birefringence is induced by the external electric field.

The obtained temperature dependence of A and B are shown in Fig. 5. There are a few noteworthy observations which follow from this figure. First, that both $A(T)$ and $B(T)$ are linear in $(T - T_w)^{-1}$. Second, that the constant T_w is the same for the A and B parameters. Finally, we have the limit,

$A(T \to 0) \to 0$. Thus, from Fig. 5, the Kerr constant obtained for the liquid is well-described by the dispersion relation in which

$$A(T) = \frac{a_1}{T - T_w}, \tag{19}$$

$$B(T) = \frac{b_1}{T - T_w} + b_2. \tag{20}$$

From these semiempirical forms the Kerr constant, $K(T, \lambda)$ with only four constants a_1, b_1, b_2, T_w can be estimated.

For small b_1 the constant T_w becomes T^* and B becomes the constant b_2. In this case $K(T, \lambda)$ becomes the simple product $K(T)K(\lambda)$ and in a particular case $b_2 = \lambda^*$ the relation holds $a_1 = \lambda^{*2} G(T - T^*)/E_s^2$. As the slope of the line or b_1 for 5CB is considerably smaller than that for M2 [Fig. 5(b)] one can expect better realisation of the product form $K(T)K(\lambda)$ in the former case.

The $K(T, \lambda)$-surfaces of 5CB and M2 fluids are shown in Fig. 6. The $K(T, \lambda)$ is a decreasing function in both ΔT and λ. Apart from the region near T_c (or small ΔT) it is fairly similar and flat for the materials considered. Thus, it is mainly the value of T^* that can cause a more significant increase in K in liquids near T_c. As mentioned above (see Fig. 3) addition of the chiral component leads to smaller $|\Delta T^*|$ which in turn results in the sequence $K(\text{M2}) > K(\text{5CB})$. For higher temperatures, this sequence reverses (i.e., the dopant lowers K) and thus, there exists a crossover line (see the dashed line in Fig. 6).

In the case of the BPII of M2 the character of the temperature dependence of K for three wavelengths at which measurements were conducted are very similar as can be seen in Fig. 4(b). In particular they are well represented by the relation given in Eq. (13). Also, the data can be approximated by the linear relation in Eq. (14) [or Eq. (15)]. Our results for different λ show that the dispersion relation in Eq. (18) describes well the $K(T, \lambda)$. However, this time we do not observe any obvious functional regularity of the temperature dependence of the A and B parameters. Nonetheless, $\sqrt{B(T)}$ can be well represented by the
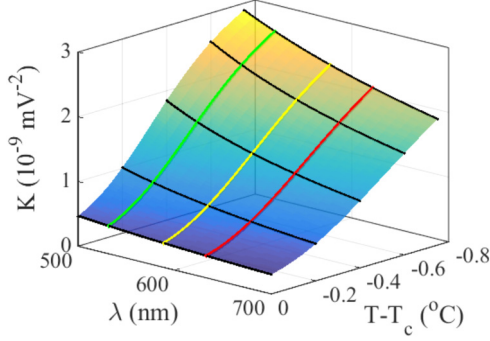
FIG. 7. Temperature and dispersion dependence of the Kerr constant, $K(T, \lambda)$, in BPII phase of M2 mixture. The color solid lines are for λ_1, λ_2, and λ_3 in Fig. 4(b). Examples of $K(\lambda)$ are denoted as solid black lines. The surface is given by relations in Eqs. (18)–(20) and the A, B parameters are represented by polynomials given in the main text.

polynomial $-201.73\Delta T^3 - 925.54\Delta T^2 - 521.9\Delta T = 227.15$. Its values are within ~ 227–305 nm which is the same order as the ~ 216 nm reported for the polymer-stabilized LC composite [35]. The second parameter decreases with temperature and can be well represented as $A(T) = (4.1707\Delta T^3 + 17.947\Delta T^2 - 3.4972\Delta T + 1.9048)10^{-7}V^{-2}$. With these relations for A and B, the $K(T, \lambda)$ of M2 BPII can be obtained with Eq. (18) and the resultant surface is shown in Fig. 7. We emphasize that the above polynomials are not unique representations of A and $\sqrt{B}$, and other functions could be used as well.

V. CONCLUSIONS

A direct and simple scheme to determine the Kerr constant (K) in optically isotropic liquid crystals has been proposed and tested. The method is based on the relation between the induced birefringence and the light intensity modulated by the electric field in the sample. The explicit expression for K is derived in terms of the two measuring voltages. In the scheme a modified IPS geometry is used which provides a sufficiently uniform longitudinal electric field. The method can operate on application of comparatively small driving voltages and can measure relatively small K values (10^{-11}mV^{-2}). Also, just as for the VFS approach [15], the method gives the ability to view the sample texture during the measurement, allowing monitoring of phase changes and the sample alignment. This feature is especially useful in studies of transition regions and temperature-narrow BPs. Another advantage is the possibility to measure directly K for different light wavelengths. A comparison of results obtained for two liquid crystals (5CB and its mixture with a chiral dopadt CE2) shows the performance and accuracy of the scheme is comparable to that of VSF.

The scheme has been used to derive some insights into the general T and λ dependence of the Kerr constant which is a difficult property to measure and a largely unexplored issue. The dependence has been investigated in liquid and BPII phases for a range of temperatures and three wavelengths. The performed measurements showed that the dispersion relation in Eq. (18) describes the experimental data very well both in the liquid phase and in the BP phase. This may mean that the

relation in Eq. (18) points to some universal behavior and can describe well the dispersion of the Kerr constant in different optically isotropic materials.

In all considered cases, the temperature dependence in isotropic liquids follows well the simple linear relationship, $1/K \sim T$ (but, the region close to the clearing temperature needs more detailed studies to confirm or disprove this behavior). In the BPII the temperature dependence of the Kerr constant can also be approximated by the linear relation which is practically equivalent to the relation proposed by Ref. [30]. The results of this work as well as results in Ref. [15] indicate however that the some departures from the linear trend are present and the K in BPII is represented well by the three parameter exponential-like formula [in Eq. (13)].

It is found that in the isotropic fluid both parameters in the dispersion relation have a simple linear T-dependence, which allows us to formulate a general form of $K(T, \lambda)$-surface with only four constants. This important and useful finding is worth further investigations (including different isotropic liquids) to establish the range of its applicability. In the case of the BPII the parameters do not display a simple T-dependence. They are however functions which can be fitted with a low-order polynomial.

APPENDIX: THE DISPERSION RELATION OF THE KERR CONSTANT

In this Appendix, the expression for the $K(T, \lambda)$ in Eq. (18) in which both parameters A, B depend of temperature is derived. The starting point is the rigorous and explicit single-band birefringence dispersion model derived by Abdulhalim [37,38] and its application to the saturated induced birefringence,

$$\Delta n_s = \frac{\sqrt{G_\parallel \lambda^2 - 1} - \sqrt{G_\perp \lambda^2 - 1}}{\sqrt{G_c \lambda^2 - 1}}. \tag{A1}$$

In the above expression $G_\parallel$, G_c, $G_\perp$, are temperature- and material-dependent parameters

$$G_\parallel = \frac{1}{\lambda^{*2}} + 2a(g_\perp + 4g_\parallel),$$

$$G_c = \frac{1}{\lambda^{*2}} - a(2g_\perp + g_\parallel), \tag{A2}$$

$$G_\perp = \frac{1}{\lambda^{*2}} + a(7g_\perp - g_\parallel), \tag{A3}$$

in which $a = 4\pi N/9$, N is the number of molecules per unit volume, λ^* as above is the wavelength of the nearest absorption band and $g_\perp$, $g_\parallel$ are the oscillator strengths perpendicular and parallel to the molecular axis, respectively. Writing Eq. (A1) in the form

$$\Delta n_s = \frac{\sqrt{G_\parallel}\sqrt{1 - \frac{1}{G_\parallel \lambda^2}} - \sqrt{G_\perp}\sqrt{1 - \frac{1}{G_\perp \lambda^2}}}{\sqrt{G_c}\sqrt{1 - \frac{1}{G_c \lambda^2}}}, \tag{A4}$$

and exploiting that $x \equiv 1/G_s\lambda^2$ $(s = \parallel, c, \perp)$ are generally small [37], we get

$$
\begin{aligned}
\Delta n_s &\cong \frac{\sqrt{G_\parallel} - \frac{1}{2\sqrt{G_\parallel}\lambda^2} - \sqrt{G_\perp} + \frac{1}{2\sqrt{G_\perp}\lambda^2}}{\sqrt{G_c} - \frac{1}{2\sqrt{G_c}\lambda^2}} \\
&= \frac{\lambda^2(\sqrt{G_\parallel} - \sqrt{G_\perp}) + \frac{1}{2}\left(\frac{1}{\sqrt{G_\perp}} - \frac{1}{\sqrt{G_\parallel}}\right)}{\sqrt{G_c}(\lambda^2 - \frac{1}{2G_c})} \quad \text{(A5)} \\
&= \frac{G^*\lambda^{*2}\lambda^2}{\lambda^2 - B}\left(1 + \frac{1}{2\sqrt{G_\perp G_\parallel}\lambda^2}\right), \quad \text{(A6)}
\end{aligned}
$$

where $G^* = (\sqrt{G_\parallel} - \sqrt{G_\perp})/\sqrt{G_c}\lambda^{*2}$ and $B = 1/2G_c$. As x is small it follows that the second term in parenthesis (A6) is

small compared to unity and from Eq. (17) one gets the expression in Eq. (18) for the Kerr constant in which both A and B are the LC material- and temperature-dependent parameters,

$$
K \cong \frac{A\lambda}{\lambda^2 - B}, \quad \text{(A7)}
$$

where $A = G^*\lambda^{*2}/E_s^2$. If in particular case $G_c = 1/2\lambda^{*2}$ or $B = \lambda^{*2}$, then G^* can be treated as G and $K(T, \lambda)$ is the product of temperature-dependent $K(T) = G\lambda^{*2}/E_s^2$ and wavelength-dependent $K(\lambda) = \lambda/(\lambda^2 - \lambda^{*2})$ parts. It is worth noting that in applying the (A7) relation the wavelength λ^* does not need to be known. Another advantage is the possibility to determine A, B with the data obtained at only two wavelengths.

[1] P. P. Crooker, *Chirality in Liquid Crystals* (Springer, Berlin, 2001), pp. 186–222.

[2] S. Chandrasekhar, *Liquid Crystals* (Cambridge University Press, Cambridge, UK, 1992).

[3] H. Kikuchi, M. Yokota, Y. Hisakado, H. Yang, and T. Kajiyama, Nat. Mater. **1**, 64 (2002).

[4] D.-K. Yang and S.-T. Wu, *Fundamentals of Liquid Crystal Devices* (John Wiley & Sons, New York, 2014).

[5] Y. Hisakado, H. Kikuchi, T. Nagamura, and T. Kajiyama, Adv. Mater. **17**, 96 (2005).

[6] L. Rao, J. Yan, S.-T. Wu, S.-i. Yamamoto, and Y. Haseba, Appl. Phys. Lett. **98**, 081109 (2011).

[7] H. Khoshsima, H. Tajalli, A. G. Gilani, and R. Dabrowski, J. Phys. D **39**, 1495 (2006).

[8] K. V. Le, S. Aya, Y. Sasaki, H. Choi, F. Araoka, K. Ema, J. Mieczkowski, A. Jakli, K. Ishikawa, and H. Takezoe, J. Mater. Chem. **21**, 2855 (2011).

[9] D. Xu, Y. Chen, Y. Liu, and S.-T. Wu, Opt. Express **21**, 24721 (2013).

[10] L. Rao, Z. Ge, S.-T. Wu, and S. H. Lee, Appl. Phys. Lett. **95**, 231101 (2009).

[11] L. Rao, H.-C. Cheng, and S.-T. Wu, J. Disp. Technol. **6**, 287 (2010).

[12] T. Iwata, K. Suzuki, H. Higuchi, and H. Kikuchi, Liq. Cryst. **36**, 947 (2009).

[13] G. Nordendorf, A. Lorenz, A. Hoischen, J. Schmidtke, H. Kitzerow, D. Wilkes, and M. Wittek, J. Appl. Phys. **114**, 173104 (2013).

[14] H.-C. Cheng, J. Yan, T. Ishinabe, C.-H. Lin, K.-H. Liu, and S.-T. Wu, J. Disp. Technol. **8**, 627 (2012).

[15] L. Tian, J. W. Goodby, V. Görtz, and H. F. Gleeson, Liq. Cryst. **40**, 1446 (2013).

[16] H.-C. Cheng, J. Yan, T. Ishinabe, and S.-T. Wu, Appl. Phys. Lett. **98**, 261102 (2011).

[17] J. Yan, H.-C. Cheng, S. Gauza, Y. Li, M. Jiao, L. Rao, and S.-T. Wu, Appl. Phys. Lett. **96**, 071105 (2010).

[18] J. Yan, M. Jiao, L. Rao, and S.-T. Wu, Opt. Express **18**, 11450 (2010).

[19] A. J. Nicastro and P. H. Keyes, Phys. Rev. A **30**, 3156 (1984).

[20] U. Singh and L. Moseley, Eur. J. Phys. **15**, 154 (1994).

[21] A. Ayriyan, E. Ayrjan, A. Egorov, G. Hadjichristov, Y. Marinov, I. Maslyanitsyn, A. Petrov, J. Pribis, L. Popova, V. Shigorin *et al.*, Phys. Wave Phenom. **24**, 259 (2016).

[22] M. Born and E. Wolf, *Principles of Optics: Electromagnetic Theory of Propagation, Interference, and Diffraction of Light* (Elsevier, Amsterdam, 2013).

[23] W. Kuczyński, D. Dardas, F. Goc, and R. Dabrowski, Ferroelectrics **244**, 191 (2000).

[24] H. Coles and B. Jennings, Mol. Phys. **36**, 1661 (1978).

[25] D. Dunmur and A. Tomes, Mol. Cryst. Liq. Cryst. **76**, 231 (1981).

[26] P. De Gennes, Mol. Cryst. Liq. Cryst. **12**, 193 (1971).

[27] N. Osiecka, Z. Galewski, and M. Massalska-Aródź, Thermochim. Acta **655**, 106 (2017).

[28] E. Bukusoglu, J. A. Martinez-Gonzalez, X. Wang, Y. Zhou, J. J. de Pablo, and N. L. Abbott, Soft Matter **13**, 8999 (2017).

[29] P. Nayek, H. Jeong, H. R. Park, S.-W. Kang, S. H. Lee, H. S. Park, H. J. Lee, and H. S. Kim, Appl. Phys. Express **5**, 051701 (2012).

[30] L. Rao, J. Yan, and S.-T. Wu, J. Soc. Inf. Disp. **18**, 954 (2010).

[31] P. R. Gerber, Mol. Cryst. Liq. Cryst. **116**, 197 (1985).

[32] G. Nordendorf, J. Schmidtke, D. Wilkes, and H. Kitzerow, J. Mater. Chem. C **5**, 518 (2017).

[33] W. Kuczyński, Mol. Cryst. Liq. Cryst. **130**, 1 (1985).

[34] C.-W. Chen, H.-C. Jau, C.-H. Lee, C.-C. Li, C.-T. Hou, C.-W. Wu, T.-H. Lin, and I. Khoo, Opt. Mater. Express **3**, 527 (2013).

[35] M. Jiao, J. Yan, and S.-T. Wu, Phys. Rev. E **83**, 041706 (2011).

[36] S.-T. Wu, Phys. Rev. A **33**, 1270 (1986).

[37] I. Abdulhalim, Mol. Cryst. Liq. Cryst. **197**, 103 (1991).

[38] I. Abdulhalim, Liq. Cryst. **33**, 1027 (2006).